united nations
educational, scientific
and cultural
organization

international atomic
energy agency

the
abdus salam
international centre for theoretical physics

SMR.1135 - 17

**THIRD WORKSHOP ON
THIN FILMS PHYSICS AND TECHNOLOGY
(8 - 24 MARCH 1999)**
including
**TOPICAL CONFERENCE ON
MICROSTRUCTURE AND SURFACE MORPHOLOGY
EVOLUTION IN THIN FILMS
(24 - 26 MARCH 1999)**

"Growth of nanocrystalline carbon films by cluster deposition: Real and computer experiments"

**Luciano COLOMBO
Universita' degli Studi di Milano-Bicocca
Dipartimento Scienza dei Materiali
Via Cozzi 53
20126 Milano
ITALY**

Growth of Nanostructured Carbon Films by Cluster Assembling

D. Donadio[1], L. Colombo[1], P. Milani[2], and G. Benedek[1]

[1] *INFM and Dipartimento di Scienza dei Materiali, Università di Milano–Bicocca, via Cozzi 53, I-20125 Milano, Italy*

[3] *INFM and Dipartimento di Fisica, Università di Milano, via Celoria 16, I-20133 Milano, Italy*

(March 17, 1999)

Abstract

The structural properties of nanostructured films obtained by deposition of supersonic beams of carbon clusters are investigated by classical molecular dynamics simulations and compared to experiments. Simulations are shown to predict how the structural properties of the deposited film depend on the actual growth protocol. In particular, it is shown that the assembling of small linear clusters can lead to the formation of random schwartzite structures.

PACS numbers: 68.55.-a, 81.05.Tp, 81.15.-z

Supersonic cluster beam deposition (SCBD) has recently emerged as a very promising technique for the growth of nanostructured carbon thin films [1–3]. When the incident energy of clusters accelerated in a supersonic expansion is small enough to prevent massive fragmentation, the aggregates retain their individuality and the resulting films present a large (but controllable) variety of morphologies. The large porosity and the presence of fullerene–like cages make these systems appealing for possible applications like gas sensing and gettering [3–6]. Moreover, the assembling of small carbon units has been suggested as possible route to the formation of negatively curved graphitic carbon (random schwartzites) [7,8].

Nanostructured SCBD films have been characterized by a variety of experimental techniques [9,10]. In particular, it has been shown that the films retain a memory of the precursor

clusters and display a disordered graphite–like character with a prevalent three–fold coordination. The films are porous with a density of ~ 1 g/cm^3. TEM analysis shows a structure consisting of closed graphitic particles and curved graphene foils embedded into an amorphous matrix. As shown in Fig.1 the film is inhomogeneous and characterized by cavities. The inhomogeneity is observed at different lenght scales up to the macroscopic one and appears to be self–affine [3].

Although experimental findings provide a detailed characterization of SCBD carbon films, it is difficult to clearly establish the relationship between the structure of the clusters (ranging from a few up to several hundreds atoms clusters) in the beam and the structural features of the resulting sample. The large variety of clusters, as well as the presence of several isomers of any given cluster with different structure and reactivity, make it difficult to predict and control the effects of cluster–cluster interaction on the substrate and the extent of rebonding during the film growth. As a consequence, the cluster assembling during the beam deposition and the structure of the resulting films at the nano– and meso–scale is still a matter of discussion [10–12].

Despite the above unclear scenario, it is nevertheless possible to identify a number of facts and key parameters governing the SCBD film growth: (i) experimental results based on ion-drift measurements [13] have shown that small carbon clusters (roughly below 40 atoms) have chain or ring structures, whereas larger clusters have the tendency to form three–dimensional cages characterized by three–fold coordination; (ii) the actual mass distribution deeply affects the final atomic–scale structure [10]; (iii) the deposition energy affects the density and the porosity of the sample; (iv) the vibrational temperature of the impinging clusters, the geometrical parameters of the beam–substrate interaction (e.g. incidence angle), as well as the energy distribution within the beam can vary in a wide range.

In this Letter we present a computer study, tailored on SCBD experiments and based on classical molecular dynamics (MD) simulations, aimed at improving our basic understanding of the SCBD growth phenomena. Although the real length and time scales of experiments fall in the mesoscopic range and are presently out of reach of MD simulations, the latter are

nevertheless scalable to the mesoscopic domain thanks to self–affinity [3] and are suggestive of the underlying mechanisms driving the growing film to form a nanostructured sample. Furthermore, through MD simulations (which provide a full atomic–scale characterization of these new materials) we have identified a number of typical issues characterizing SCBD experiments. By means of the present simulations, we have established a rational link between the physical properties of the grown films and the beam features.

The present computer–intensive investigation has been carried out by classical MD simulations based on the many–body Tersoff interaction potential [14]. We made use of an improved version of this potential which better models the effects of the local environment on the atom–atom interactions [15].

The deposition of clusters was performed with a normal incidence and a uniform in–plane distribution on a (001)–oriented periodically repeated diamond substrate. The substrate temperature was fixed at 300 K by velocity rescaling, while the dynamics of the free surface was left unperturbed (i.e. no rescaling was operated for the outmost atoms) in order to avoid artifacts during the early stages of beam–substrate (then beam–film) interaction. All computer experiments discussed here were performed with mono–energetic cluster beams with a vibrational temperature of T_v=500 K. The deposition energy E_d was tuned in the interval 0.1 eV/atom $< E_d <$ 1.0 eV/atom. The values of T_v and E_d have been chosen according to the typical source conditions of a supersonic cluster beam produced by a pulsed plasma source [1–3,10]. By using a time–step δt of 0.5 fs, we deposited up to $\sim 10^4$ atoms (corresponding to a thickness of the deposited film of $\sim$ 50 Å). These parameters correspond to a very high deposition rate, varying in the range 10^{24}–10^{25} atoms/s/cm^2. This is to be compared to the typical experimental values of 10^{17}–10^{18} atoms/s/cm^2. Despite this difference, the theoretical deposition rate is low enough to warrant that the next cluster impact occurs after a full relaxation of the previous one. Special care has been taken in selecting the configuration of carbon clusters in the beam. The precursors for the film growth have been shaped according to experimental ion–drift measurements [13]: while clusters with more than 40 atoms have been arranged in fullerene–like cages, smaller clusters (containing

up to 23 atoms) have been shaped as either linear chains (odd number of carbon atoms) or closed rings (even number of carbon atoms). No clusters with intermediate size (from 24 to 45 atoms) have been inserted in the beams, according to Ref. [16].

We first consider the role played by the mass distribution in the beam. To this aim we performed two different simulations where a bi–modal distribution was assumed. In both cases we selected a beam consisting of clusters of size 1–23 atoms and 46–120 atoms with a relative intensity of 5:1 and 1:10, respectively. The respective snapshots of the grown samples are reported in Fig.2(a) and (b). In these simulations the substrate was quite extended (deposition area of 53Å×53Å), as requested by the relatively large dimensions of the deposited precursors. We selected $E_d = 0.1$ eV/atom. Sample (a) resulted to have a density of 0.85 gr/cm in substantial good agreement with real SCBD films [9]. Furthermore, sample (a) is homogeneous showing only very small density fluctuations in the bulk region when measured along the growth axis. The fullerene structures, still detectable in the film, are connected by an amorphous matrix characterized by three–fold coordination and hexagonal bond rings. The overall structure is far dominated by three–fold coordination, in agreement with the experiments [9,10].

By reversing the relative occurrence of small and big precursors we obtained a different kind of film. Indeed sample (b) shows intriguing structural properties. While the overall disorder in the bond network is apparent, the presence of nearly unaffected fullerene cages is easily recognized. The random stacking of fullerene precursors gives rise to a locally–structured, stress–free, porous film with a low density (0.79 g/cm^3). Sample (b), unlike the former case, is no longer homogeneous. Rather it displays density fluctuations of about 20%, which we attributed to a local gettering effect of fullerenes over smaller clusters. Again, the atomic coordination is definitely graphite–like with 87% of atoms showing three–fold coordination. We also collected the ring statistics following the shortest–path criterion by Franzblau [17]. Although the hexagonal rings dominate we computed twice as much pentagonal rings than heptagonal ones. The resulting film is therefore characterized by fullerene–like closed structures, rather than graphite–like foils, most connections occurring

through few 4–coordinated atoms.

The above simulations proved that fullerene cages are nearly unaffected by deposition process, since nearly no fragmentation was observed. Therefore, we decided to study the role played by smaller and more fragile clusters. In particular, we considered the role played by E_d. We simulated a cluster beam deposition with a unimodal mass distribution containing small clusters of 2 to 10 atoms, with average cluster size equal to 6 (Fig.3). Single carbon atoms were included in the beam as well. The simulation cell area of the substrate was in this case of 25Å×25Å. Three snapshots of the grown films corresponding to E_d=0.1 eV/atom (sample (c)), E_d=0.5 eV/atom (sample (d)), and E_d=1.0 eV/atom (sample (e)) are shown in Fig.3. It is apparent that the sample (c), obtained with the lowest deposition energy, is highly porous, while a much denser sample is obtained at higher deposition energy. The fraction of occupied volume [18] ranges from 22% for sample (c), to 32% for sample (d), to 34% of sample (e). The corresponding surface specific area is $\sim$ 1.5 10^3 m^2/g, remarkably larger than in carbon foams systems [19]. The corresponding mass density is 0.92, 1.45 and 1.56 g/cm^2, respectively. The color code showing local atomic coordination (see figure caption) proves that the grown samples are dominated by three-fold coordination, with a fraction of sp^2 network sites of about 70% in all cases. This is consistent with the graphite–like character observed experimentally [2,3]. Samples (c) and (d) also display a sizeable percentage (about 25%) of two-fold coordinated atoms, mainly located at the surface of the internal cavities. The presence of such linear structures has been recently found by Raman measurements in SCBD films [10]. With regard to the ring statistics, we found a majority of hexagonal (18% 33%) and heptagonal (14%–18%) rings, while at variance with samples (a,b) pentagonal rings are nearly absent. This statistics indicates that open structures (e.g. graphene sheets with a negative curvature) are preferred, as actually seen in Fig.3. In particular, sample (c) clearly exhibits a random pore structure typical of random schwartzites [7,8]. Despite their porosity, the structures are rather stable with a binding energy $\sim$ 0.8 eV/atom smaller than that of diamond. Robust thermal annealing operated up to 2000 K on the as–grown samples did not significantly affect the overall atomic

architecture. After annealing, the macroscopic elastic stress parallel to the growth direction of samples (c) and (d) was found to be slightly compressive ($\sim$ 0.5 GPa) and mainly located at the film/substrate interface. All samples are stress-free along the growth direction. The absence of stress is in good agreement with experiments proving that SCBD films as thick as 30 μm can be grown without delamination [3].

In summary, classical MD simulations tailored on real experiments have been used to characterize and to predict the growth of carbon thin films by supersonic cluster beam deposition. Simulations suggest that a beam containing very small clusters with low incident energy per atom, can produce porous films with random schwartzites structures. This new synthetic routes based on SBCD are currently being investigated.

Work supported by INFM under the Advanced Research Project CLASS. We thank S. Gialanella for providing us TEM pictures and P. Piseri and M. Barborini for film deposition.

REFERENCES

[1] P. Milani and S. Iannotta, "Cluster beam synthesis of nanostructured materials", Springer Series in Cluster Physics (Springer Verlag, Berlin, 1999).

[2] P. Milani *et al.*, J. Appl. Phys. **82**, 5793 (1997).

[3] P. Milani *et al.*, Europ. J. Phys. D (1998), in press.

[4] C. Niu *et al.*, Appl. Phys. Lett. **70**, 1480 (1997).

[5] C. Nudetzenadel *et al.*, Electrochem. Solid State Lett. 2, 1 (1998).

[6] A.C. Ferrari *et al.*, Europhys. Lett. (1999), in press.

[7] T. Lenosky *et al.*, Nature **355**, 333 (1992).

[8] S. Spadoni *et al.*, Europhys. Lett. **39**, 269 (1998).

[9] C. Lenardi *et al.*, J. Appl. Phys. (1999), in press.

[10] E. Barborini *et al.*, Chem. Phys. Lett. **300**, 633 (1999).

[11] A. Canning, G. Galli and J. Kim, Phys. Rev. Lett. **78**, 4442 (1997).

[12] A. Perez *et al.*, J. Phys. D: Appl. Phys. **30**, 709 (1997).

[13] G. van Helden, N. Gotts, and M. Bowers, Nature **363**, 60 (1993).

[14] J. Tersoff, Phys. Rev. B**39**, 5566 (1989).

[15] D. Mura, L. Colombo, R. Bertoncini, and G. Mula, Phys. Rev. B **58**, 10357 (1998).

[16] E.A. Rohlfing, D.M. Cox, and A. Kaldor, J. Chem. Phys. **81**, 3322 (1984).

[17] D.S. Franzblau, Phys. Rev. B**44**, 4925 (1991).

[18] The fraction of occupied volume has been estimated by construction of Voronoi polyhedra, whose volume was assigned to "occupied space" provided that the selected polyhedra contained a carbon atom.

[19] W.R. Even Jr. and D.P. Gregory, Mat. Res. Soc. Bull. **XIX**, 29 (1994).

FIGURES

FIG. 1. TEM micrograph of a cluster assembled film showing large pores and fullerene–like particles embedded in an amorphous matrix. The film has been deposited with a cluster mass distribution described in the text and a deposition energy of 0.1 eV/atom.

FIG. 2. Atomic structure of amorphous film obtained by deposition of beams with bi–modal mass distribution in the range 1–23 atoms and 46–120 atoms with relative weight 5:1 (sample (a)) and 1:10 (sample (b)), respectively. The color code indicate the atomic stress. Blue tensile stress; red: compressive stress.

FIG. 3. Atomic structure of amorphous film obtained by deposition of beams with uni–modal mass distribution ranging from 1 to 9 atoms/cluster. The deposition energy was E_d=0.1 eV/atom (sample (c)), E_d=0.5 eV/atom (sample (d)), E_d=1.0 eV/atom (sample (e)). A color code shows the local atomic coordination. Gray: one–fold coordinated atoms; yellow: two–fold coordinated atoms; green: three–fold coordinated atoms; red: four–fold coordinated atoms.


240 nm

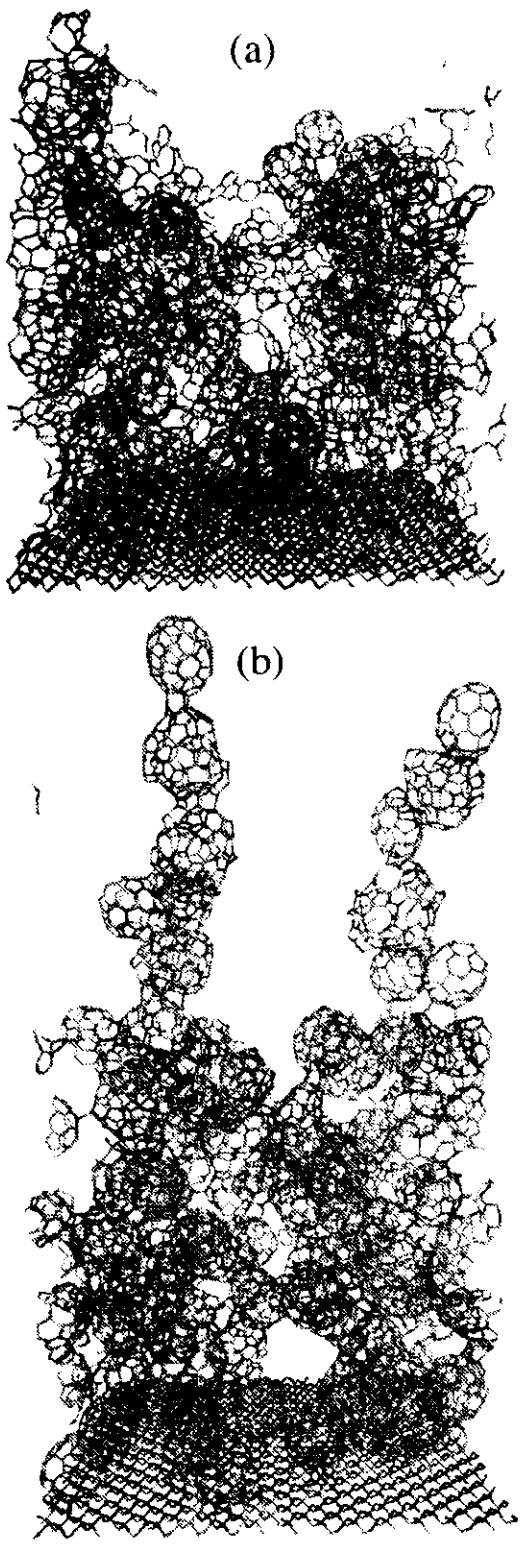
(a)
(b)

(c)

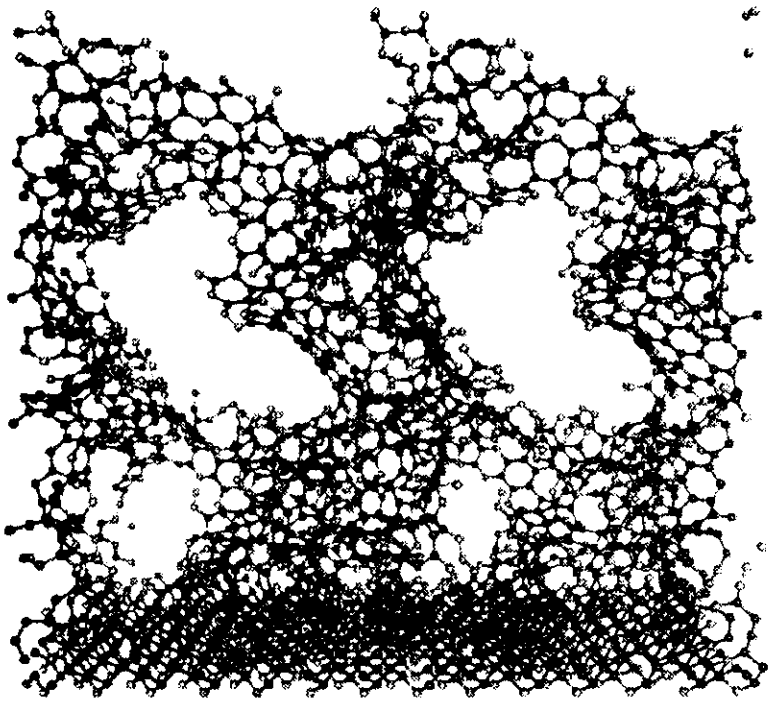

(d)

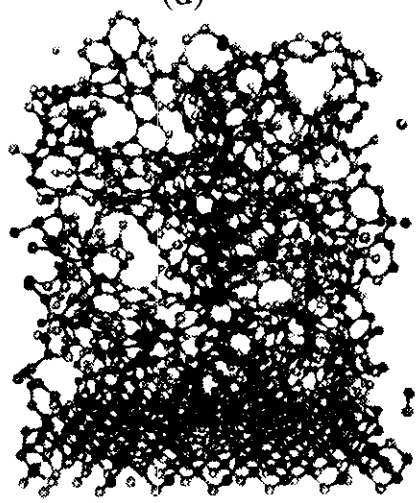

(e)

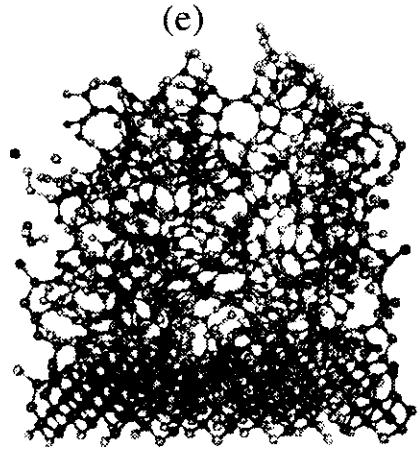

3rd WORKSHOP ON THIN FILMS PHYSICS AND TECHNOLOGY

ICTP 8-26 MARCH 1999

TOPICAL CONFERENCE ON: "MICROSTRUCTURE AND SURFACE MORPHOLOGY EVOLUTION IN THIN FILMS"

"GROWTH OF NANOCRYSTALLINE CARBON FILMS BY CLUSTER DEPOSITION: REAL AND COMPUTER EXPERIMENTS"

LUCIANO COLOMBO - INFM and DEPT. MATERIALS SCIENCE
Univ. Milano-Bicocca
E-mail: LUCIANO.COLOMBO@MATER.UNIMI.IT

Co-workers:
DAVIDE DONADIO } Theory / Simulation
MATTEO BOGANA }
PAOLO MILANI } Expt.
GIORGIO BENEDEK } Supervisor INFM project "CLUSTER ASSEMBLED MATERIALS"

- OUTLINE

  - STRUCTURAL PROPERTIES OF SUPERSONIC CLUSTER BEAMS DEPOSITED ON A SUBSTRATE
  - CLASSICAL MOLECULAR DYNAMICS
  - EXPERIMENT-TAILORED SIMULATIONS
  - KEY PARAMETERS : DEPOSITION ENERGY
    MASS DISTRIBUTION
    THERMAL DISTRIBUTION
    DEPOSITION RATE
  - SURFACE ROUGHNESS

- PRESENTATION

  - 1-HOUR LECTURE : Introduction to MD simulations
  - 2-HOUR LECTURE : Film growth and characterization

- **WHAT IS A MD SIMULATION ?**

  - Let $\{ \vec{x}_i \;\; i=1,\dots,N \}$ be the set of position vectors of N particles

  - Let $U = U(\vec{x}_1, \vec{x}_2, \dots, \vec{x}_N)$ be a given particle-particle interaction potential (it does not depend on particle velocities)

  - Then: $\vec{F}_i = -\vec{\nabla}_i U$ is the force acting on the i-th particle ⟶ THE MICROSTATE EVOLVES IN TIME

(A)

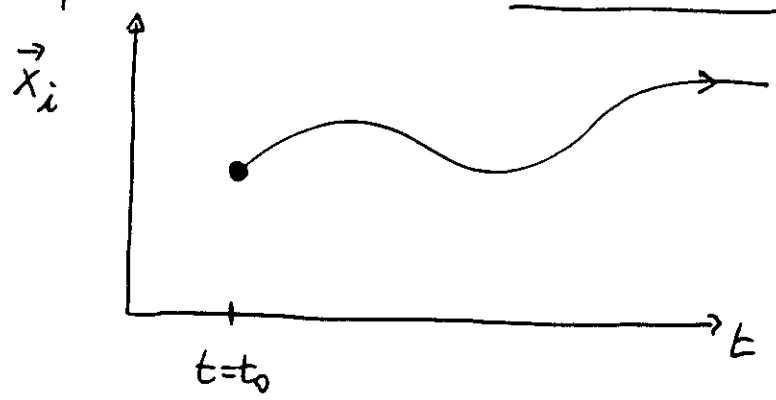

"mechanical" interpretation

or

(B)

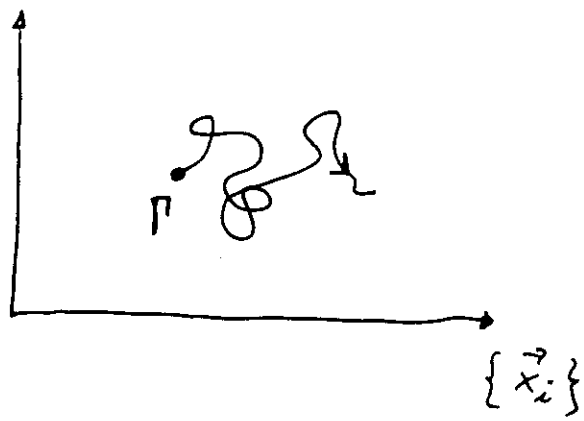

"statistical mechanics" interpretation

(A) → atomic trajectories, film growth animation, equilibrium configuration, ...

(B) → ensemble (or time) averages of microscopic physical observables ⟶ macroscopic properties

• ACTUAL NUMERICAL IMPLEMENTATION OF MD

- Discretization of time evolution

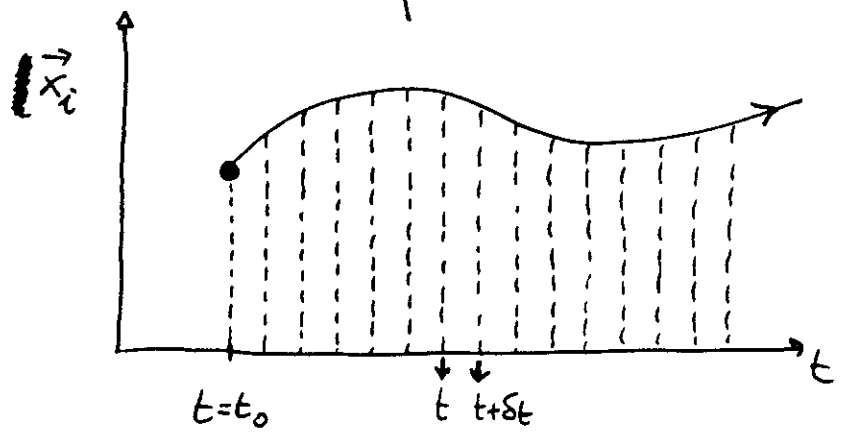

δt = TIME-STEP $\simeq$ 10^{-15} s (!)

- Between t and $t+\delta t$ we assume that the force

$$\vec{F}_i(t) = -\vec{\nabla}_i U\left[\vec{x}_1(t), \vec{x}_2(t), \dots, \vec{x}_N(t)\right]$$

is constant

- So, between t and $t+\delta t$ the particles is linearly and uniformly accelerated:

$$\vec{x}_i(t_0+\delta t) = \vec{x}_i(t_0) + \dot{\vec{x}}_i(t_0)\,\delta t + \frac{1}{2}\ddot{\vec{x}}_i(t_0)\,\delta t^2$$

$$\dot{\vec{x}}_i(t_0+\delta t) = \dot{\vec{x}}_i(t_0) + \ddot{\vec{x}}_i(t_0)\,\delta t$$

$$\ddot{\vec{x}}_i(t_0) = \vec{F}_i(t)/m_i = \frac{-\vec{\nabla}_i U\left[\vec{x}_1(t), \dots, \vec{x}_N(t)\right]}{m_i}$$

NOTE#1 : we impose Newton-like dynamics

NOTE#2 : the above differential equations are solved by finite-difference methods

- The first (simplified) MD scheme:

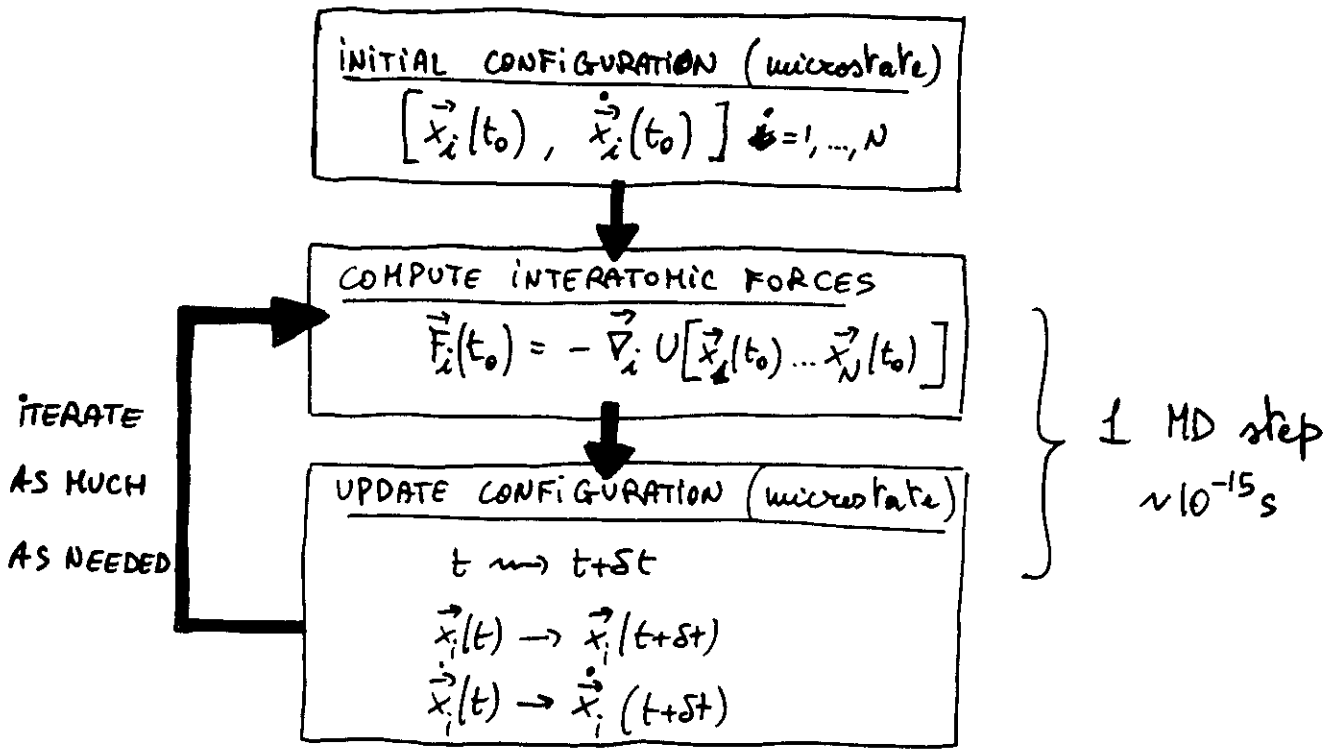

- So far, we have not yet defined any thermodynamical ensemble

  temperature pressure stress ...

- In fact, Newton equations of motion are solved with suitable thermodynamical constraints so that the resulting microstate evolution belongs to the desired ensemble.

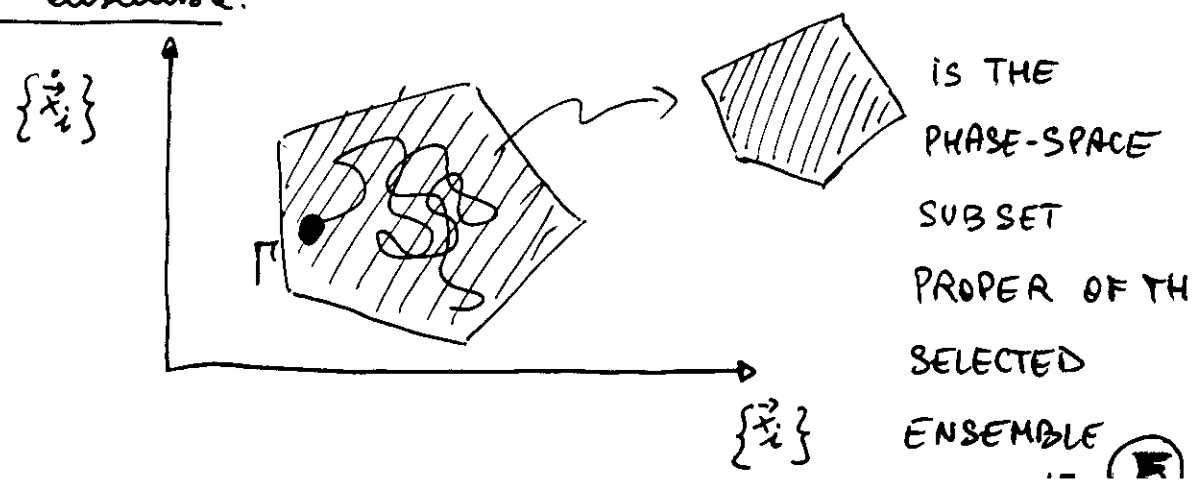

- Example: temperature control (velocity rescaling)

* at equilibrium: $\frac{1}{2}\sum_{i=1}^{N} m_i \dot{x}_i^2 = \frac{3}{2} N k_B T$

$$T = \frac{1}{3Nk_B}\sum_{i=1}^{N} m_i \dot{x}_i^2$$

* let $T_{thermostat}$ the temperature of a reference thermostat

* then, at time t we can write:

$$T(t) = \frac{1}{3Nk_B}\sum_{i=1}^{N} m_i \dot{x}_i^2(t)$$ ensemble (system) temperature

$$\boxed{\frac{T_{thermostat}}{T(t)} = \alpha} \Rightarrow \tilde{\dot{x}}_i(t) = \sqrt{\alpha}\, \dot{x}_i(t)$$

* so, by rescaling the velocities of the particles we obtain:

$$\tilde{T}(t) = \frac{1}{3Nk_B}\sum_{i=1}^{N} m_i \alpha \dot{x}_i^2(t)$$

$$= \alpha \frac{1}{3Nk_B}\sum_{i=1}^{N} m_i \dot{x}_i^2(t)$$

$$= \alpha\, T(t)$$

$$= \frac{T_{thermostat}}{T(t)}\, T(t) = T_{thermostat}$$

- More sophisticated (i.e. more rigorous) methods exist to control temperature, pressure, stress, ...

  temperature ⟶ Nosé-Hoover thermostat

  pressure (hydrostatic) → Andersen piston

  stress ⟶ Parrinello-Rahman method

- The resulting <u>complete MD scheme</u> is:

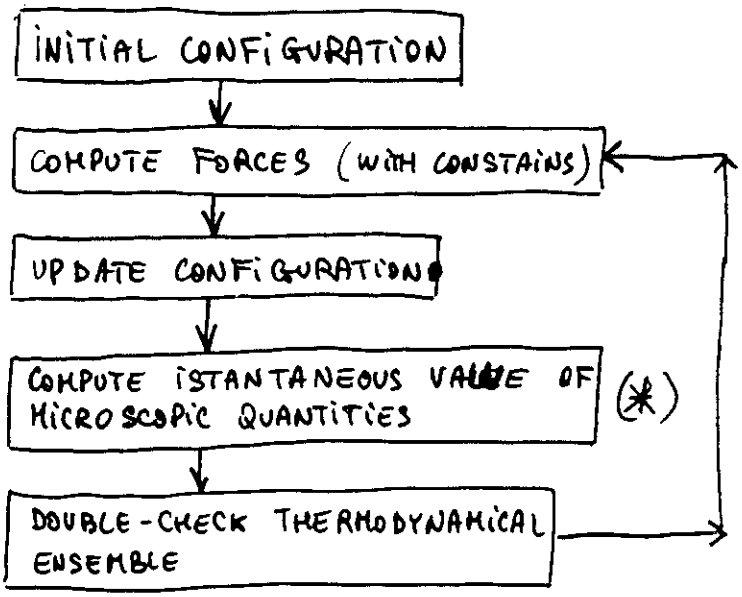

1 MD step

$\delta t \sim 10^{-15}\,s$

where (*) means:

$$\langle \vartheta \rangle_{MACRO} = \frac{1}{T}\int_{t_0}^{t_0+T} \vartheta(\Gamma(t))\,dt \simeq \frac{1}{N_{st}}\sum_{n=1}^{N_{st}} \vartheta(\Gamma(t_0+n\delta t))$$

ISTANTANEOUS VALUE

assuming that <u>ergodicity holds</u>.

- **OPEN PROBLEMS**

(1) INTERATOMIC POTENTIAL

* This work: **TERSOFF MANY-BODY CLASSICAL POTENTIAL**

- Tersoff, PRB 39, 5566 ('89)
- Muza et al., PRB 58, 10357 ('98)

$$U = \frac{1}{2} \sum_{i \neq j} V_{ij}$$

$$V_{ij} = f_C(x_{ij}) \left[f_R(x_{ij}) + b_{ij} f_A(x_{ij}) \right]$$

- CUT-OFF FUNCTION
- TWO-BODY STERIC REPULSION
- TWO-BODY COVALENT ATTRACTION

b_{ij} = MEASURES AND WEIGHTS THE BOND-ORDER
(it is an ENVIRONMENT-DEPENDENT TERM)

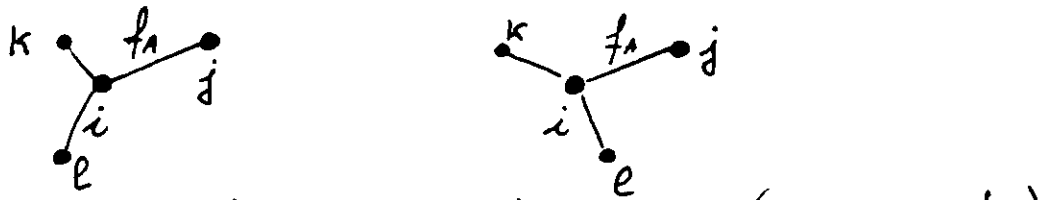

DIFFERENT ENVIRONMENTS (i.e. varying b_{ij})

↓

DIFFERENT COVALENT
i-j ATTRACTION

* Tersoff potential good for:
- diamond vs. graphite pts.
- a-C
- SiC
- low computational workload

↓

LARGE-SCALE SIMULATIONS

(2) SIMULATION TECHNICALITIES

This work : - periodic boundary conditions

- linked cells / Verlet lists
- velocity-rescaling for T-control
- Large-scale simulations :

$\sim 10^6$ time-steps

$\sim 10^4$ atoms